Optical Behaviors and Electronic Properties of Mo_2–Mo_2 Mixed-Valence Complexes within or beyond the Class III Regime: Testing the Limits of the Two-State Model

Ying Ning Tan,[1,†] Tao Cheng,[1,†] Miao Meng,[1] Yu Yu Zhang,[1] Chun Y. Liu[1,2,*], Mei Fang Sun,[2] Yu Zhang,[2] Paul J. Low[3,*]

Supporting Information for Review

Figure S1. ^{1}H NMR spectra for the complex [**O_2–O_2**].

Figure S2. ^{1}H NMR spectra for the complex [**OS–OS**].

Figure S3. ^{1}H NMR spectra for the complexes [**S_2–S_2**].

Figure S4. Spectra of electron paramagnetic resonance (EPR) for the cations [**O_2–O_2**]$^+$, [**OS–OS**]$^+$ and [**S_2–S_2**]$^+$ in CH_2Cl_2 solutions.

Table S1. Crystallographic data of the complexes [**OS–OS**] and [**S_2–S_2**].

Table S2. Selected bond distances (Å) and angles of the complex [**OS–OS**].

Table S3. Selected bond distances (Å) and angles of the complex [**SS–SS**].

Figure S5. Vis-Near-IR spectra of neutral [**O_2–O_2**] and cation [**O_2–O_2**]$^+$ in CH_2Cl_2 solutions.

Figure S6. Vis-Near-IR spectra of neutral [**OS–OS**] and cation [**OS–OS**]$^+$ in CH_2Cl_2 solutions.

Figure S7. Vis-Near-IR spectra of neutral [**S_2–S_2**] and cation [**S_2–S_2**]$^+$ in CH_2Cl_2 solutions.

Figure S8. Vis-Near-IR spectra of the cation [**O_2–O_2**]$^+$ in various solvents including THF, MeCN and DMF.

Figure S9. Vis-Near-IR spectra of the cation [**OS–OS**]$^+$ in various solvents including THF, MeCN and DMF.

Figure S10. Vis-Near-IR spectra of the cation [**S_2–S_2**]$^+$ in various solvents including THF, MeCN and DMF.

Figure S11. The key frontier molecular orbitals for the computational models of [**OO–OO**]$^+$, [**OS–OS**]$^+$ and [**SS–SS**]$^+$.

***Note for Figure** 11.*

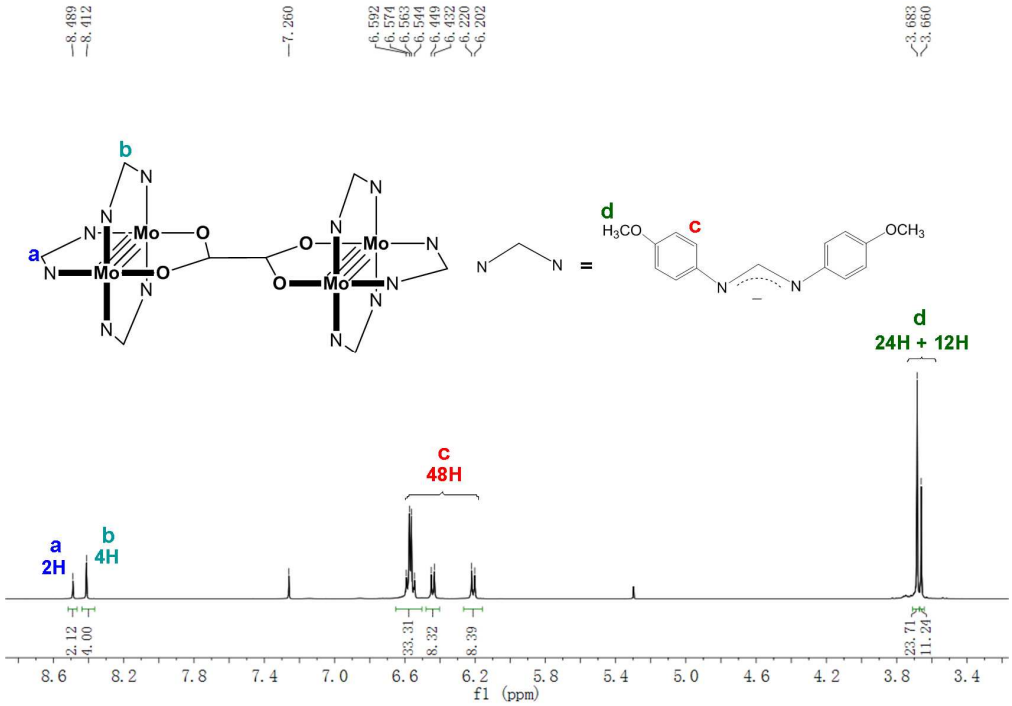

Figure S1. ^{1}H NMR spectra for the complex [$\mathbf{O_2}$–$\mathbf{O_2}$] in Chloroform-*d*.

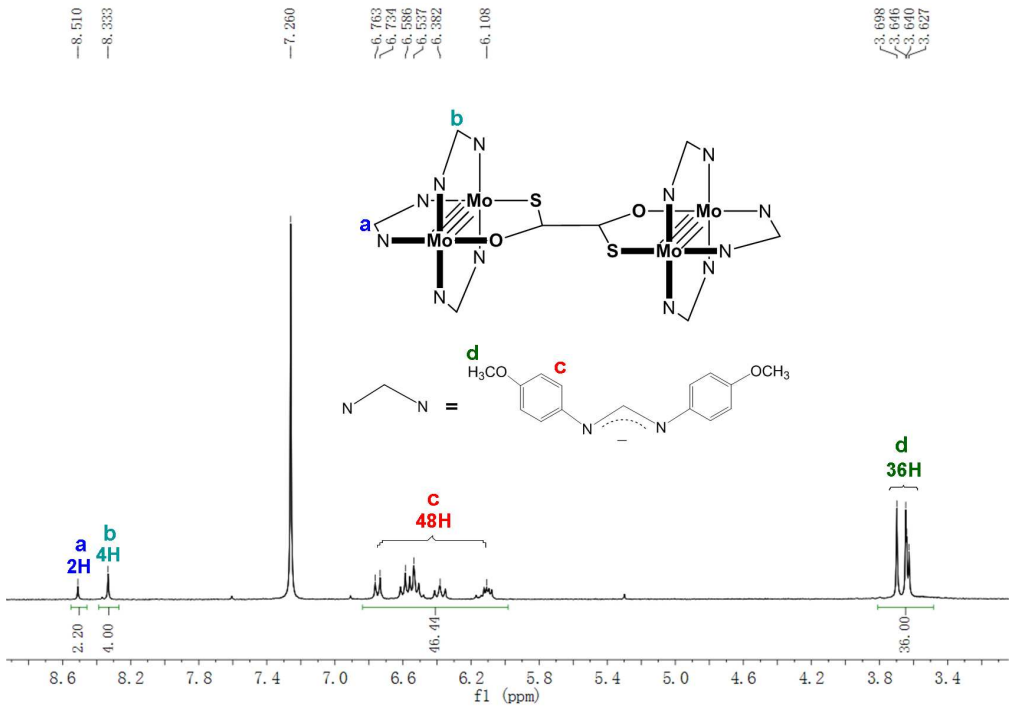

Figure S2. ^{1}H NMR spectra for the complex [**OS**–**OS**] in Chloroform-*d*.

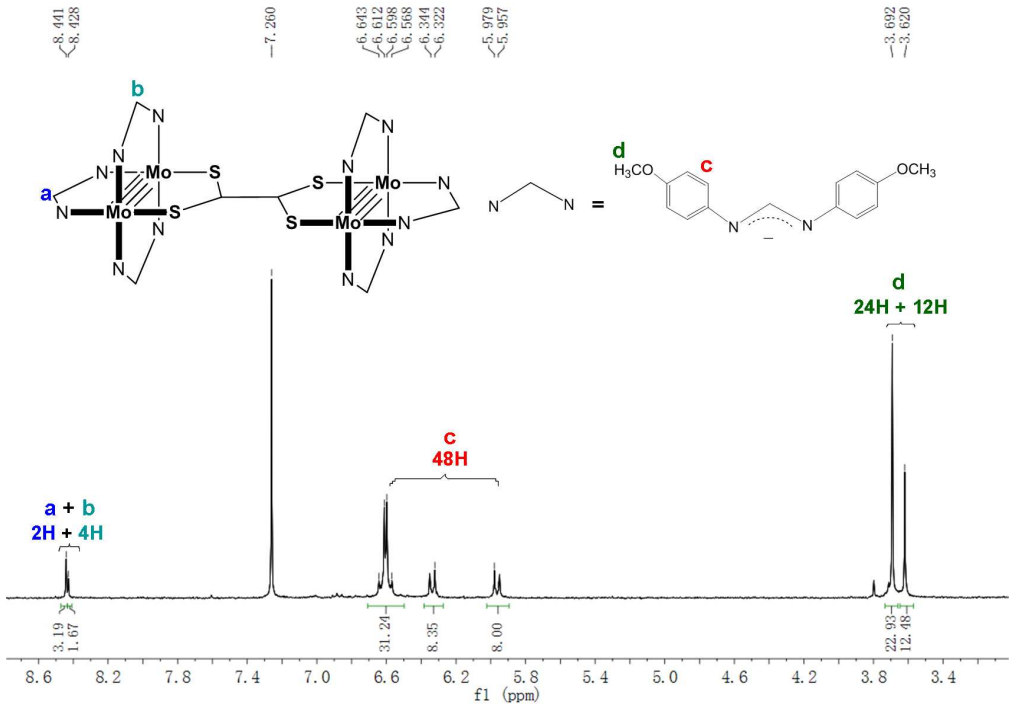

Figure S3. ^{1}H NMR spectra for the complex [$\mathbf{S_2–S_2}$] in Chloroform-*d*.

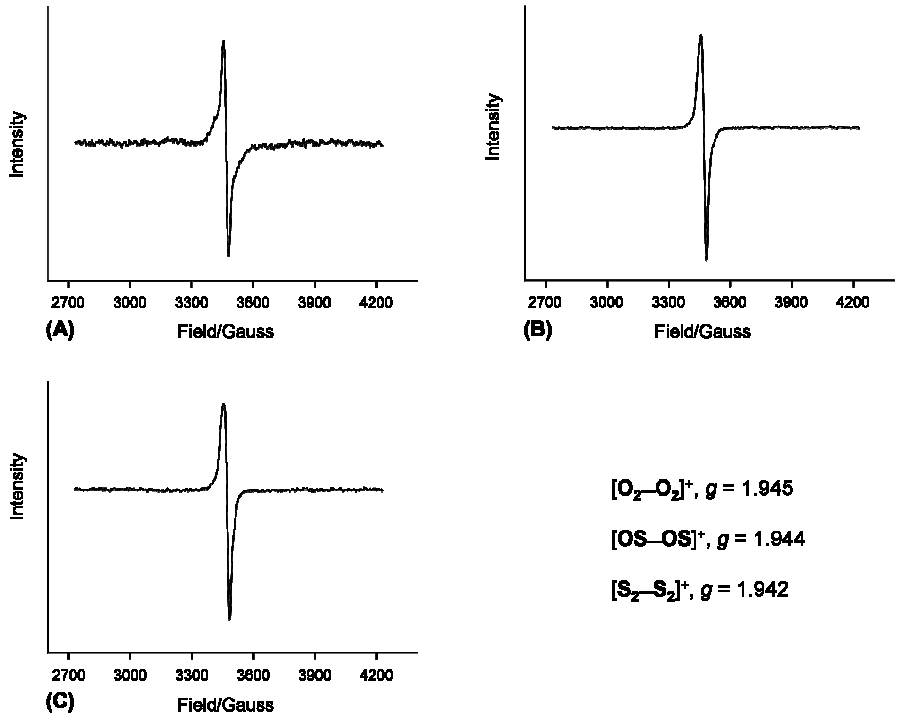

Figure S4. Spectra of electron paramagnetic resonance (EPR) for the cations $[\mathbf{O_2–O_2}]^+$ (A), $[\mathbf{OS–OS}]^+$ (B) and $[\mathbf{S_2–S_2}]^+$ (C) in CH_2Cl_2 solutions at 110 K.

Table S1. Crystallographic data for the complexes [**OS–OS**] and [$\mathbf{S_2–S_2}$]

	[OS–OS]·4CH$_2$Cl$_2$	**[S$_2$–S$_2$]·3CH$_2$Cl$_2$**
formula	$C_{96}H_{92}Mo_4N_{12}O_{14}S_2Cl_8$	$C_{95}H_{86}Mo_4N_{12}O_{12}S_4Cl_6$
fw	2369.30	2312.45
space group	$P\bar{1}$	$P\bar{1}$
a(Å)	11.2150(3)	15.0656(5)
b(Å)	15.2523(6)	15.3202(4)
c(Å)	16.1339(5)	22.8869(7)
α(deg)	97.592(3)	103.864(3)
β(deg)	108.623(3)	101.841(3)
γ(deg)	98.590(3)	90.522(2)
V(Å^3)	2537.88(16)	5010.0(3)
Z	1	2
T (K)	173	173
d_{calcd}(g/cm^3)	1.550	1.533
μ(mm^{-1})	6.828	6.788
R_1[a]	0.0646	0.0480
wR_2[b]	0.1825	0.1398

[a] $R_1 = \Sigma||F_o| - |F_c||/\Sigma|F_o|$. [b] $wR_2 = [\Sigma[w(F_o^2 - F_c^2)^2]/\Sigma[w(F_o^2)^2]]^{1/2}$

Table S2. Selected bond distances (Å) and angles (deg) for the complex [**OS–OS**].

Mo(1)-Mo(2)	2.099(6)
Mo(1)-N(1)	2.136(4)
Mo(1)-N(3)	2.148(6)
Mo(1)-N(5)	2.140(5)
Mo(2)-N(2)	2.165(6)
Mo(2)-N(4)	2.136 (6)
Mo(2)-N(6)	2.164(5)
Mo(2)-O(7)	2.082(4)
Mo(1)-S(1)	2.458(2)
C1－C2	1.476(8)
Mo_2⋯⋯Mo_2	7.354(7)
torsion angle	0.22

Table S3. Selected bond distances (Å) and angles (deg) for the complex [**SS–SS**].

Mo(1)-Mo(2)	2.101(6)	Mo(3)-Mo(4)	2.109(5)
Mo(1)-N(1)	2.137(5)	Mo(3)-N(11)	2.145(5)
Mo(1)-N(3)	2.161(5)	Mo(3)-N(7)	2.152(5)
Mo(1)-N(5)	2.156(5)	Mo(3)-N(9)	2.158(5)
Mo(2)-N(2)	2.169(5)	Mo(4)-N(8)	2.155(5)
Mo(2)-N(4)	2.143(5)	Mo(4)-N(10)	2.131(5)
Mo(2)-N(6)	2.156(5)	Mo(4)-N(12)	2.142(5)
Mo(1)-S(1)	2.421(4)	Mo(3)-S(3)	2.415(3)
Mo(2)-S(2)	2.435(2)	Mo(4)-S(4)	2.421(1)
C1－C2	1.454(7)	Mo_2·····Mo_2	7.881(6)
torsion angle	21.53		

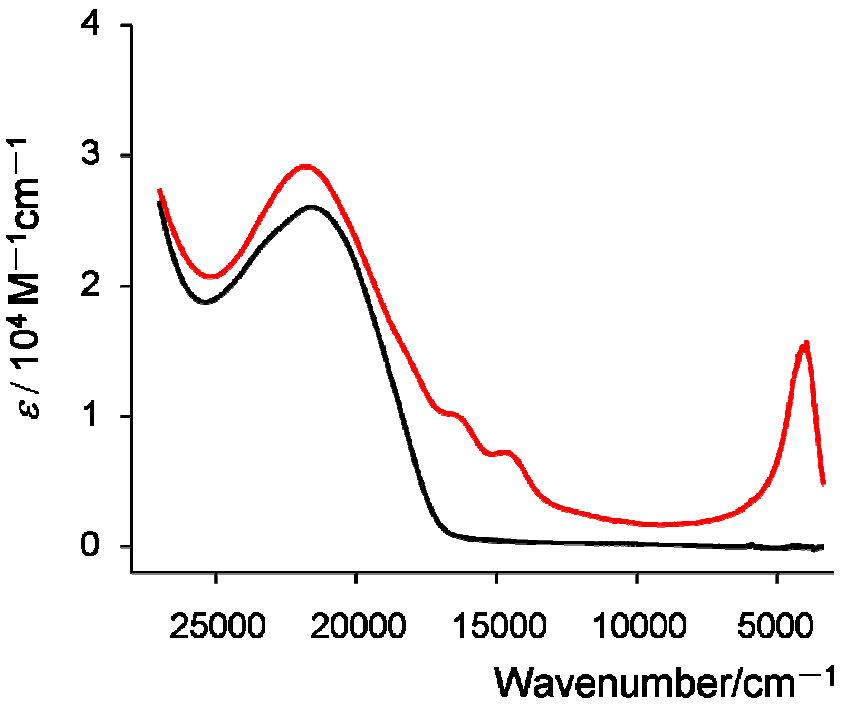

Figure S5. Vis-Near-IR spectra of neutral [**O₂–O₂**](black) and cation [**O₂–O₂**]$^{+}$(red) in CH_2Cl_2 solutions.

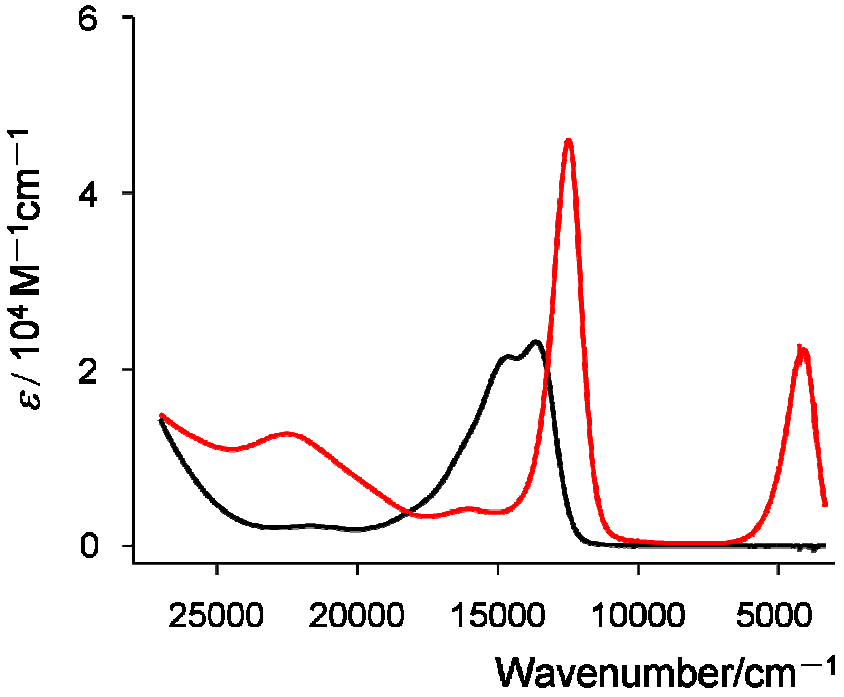

Figure S6. Vis-Near-IR spectra of neutral [**OS–OS**](black) and cation [**OS–OS**]$^{+}$ in CH_2Cl_2 solution.

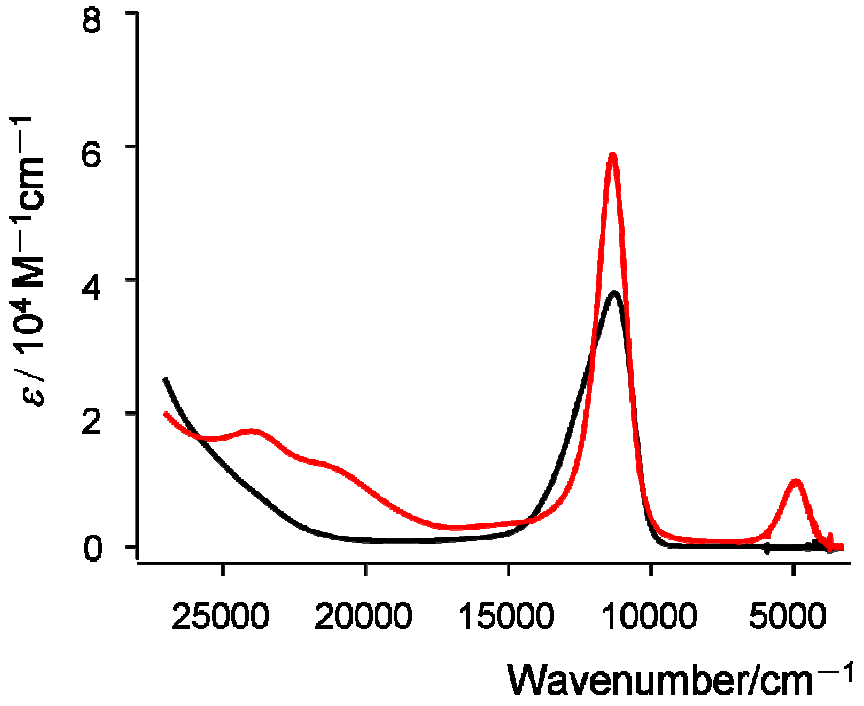

Figure S7. Vis-Near-IR spectra of the cation $[\mathbf{S_2}–\mathbf{S_2}]^+$ in CH_2Cl_2 solution.

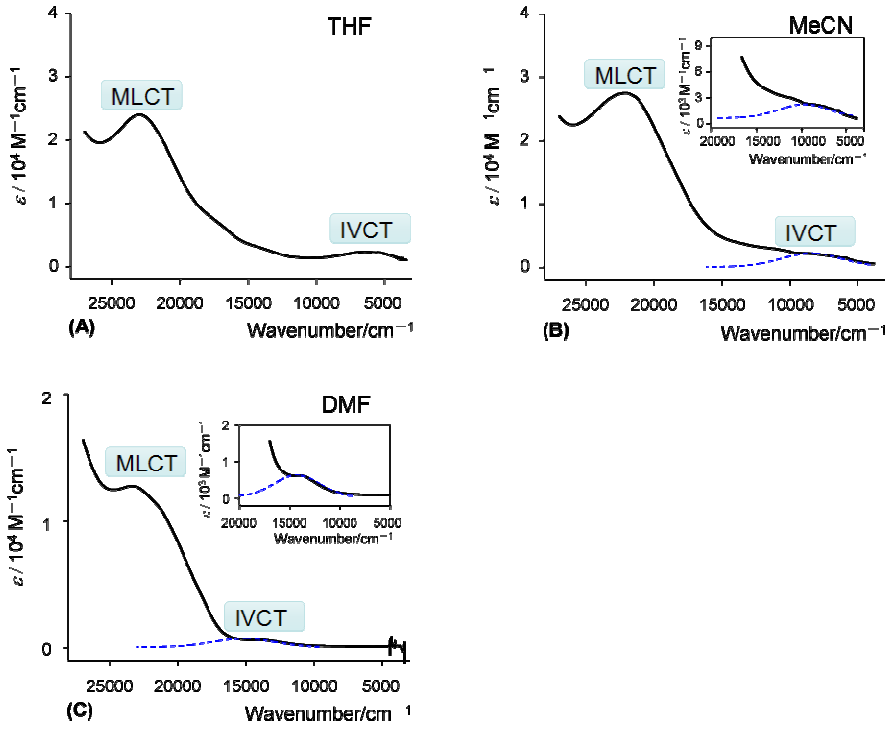

Figure S8. Vis-Near-IR spectra of the cation $[\mathbf{O_2}–\mathbf{O_2}]^+$ in various solvents including THF (A), MeCN (B) and DMF (C).

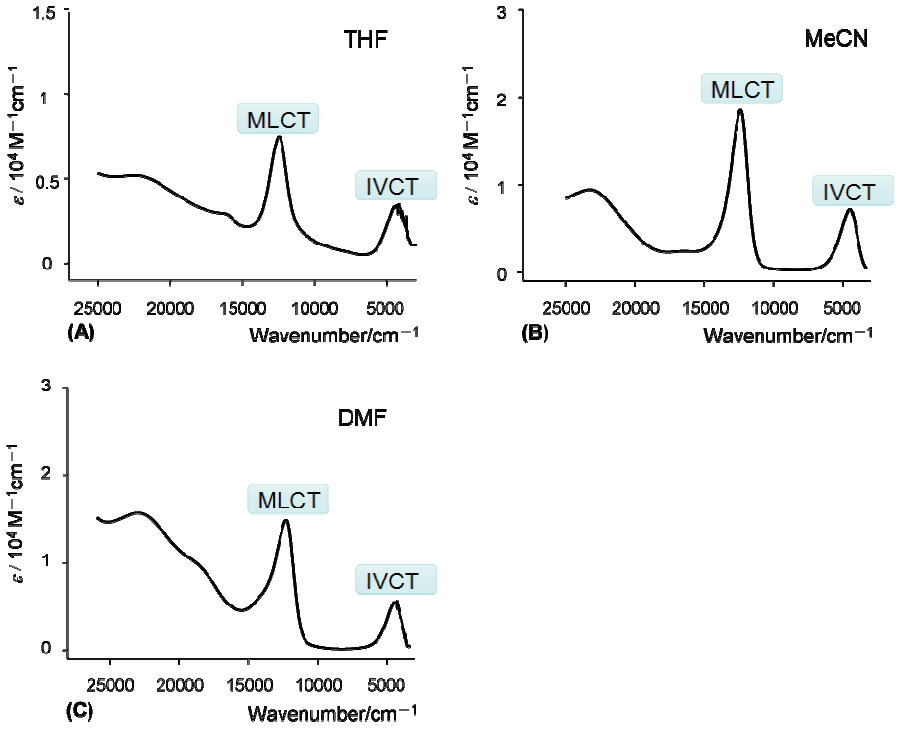

Figure S9. Vis-Near-IR spectra of the cation $[\mathbf{OS–OS}]^+$ in various solvents including THF (A), MeCN (B) and DMF (C).

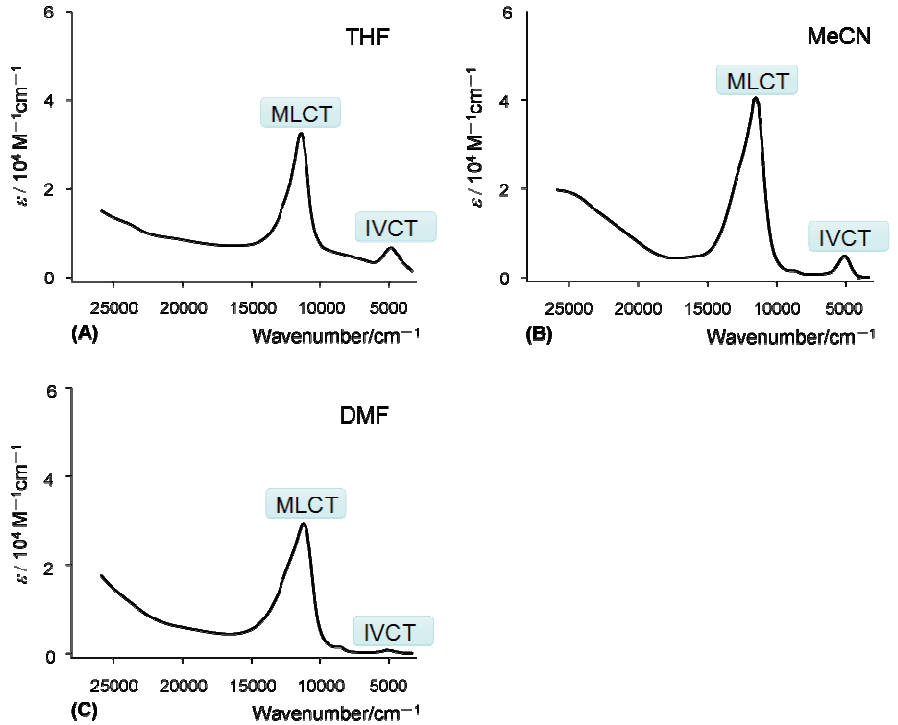

Figure S10. Vis-Near-IR spectra of the cation $[\mathbf{S_2–S_2}]^+$ in various solvents including THF (A), MeCN (B) and DMF (C).

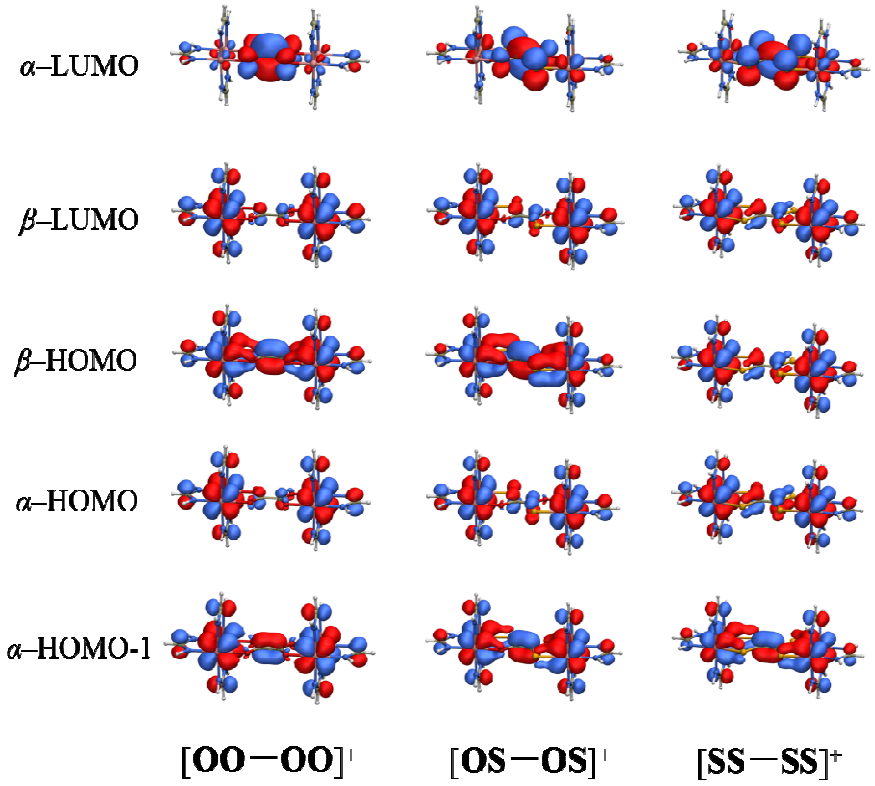

Figure S11. The key frontier molecular orbitals for the computational models of $[\mathbf{OO–OO}]^+$, $[\mathbf{OS–OS}]^+$ and $[\mathbf{SS–SS}]^+$.

Note for Figure 11: The adiabatic potential surfaces are generated by calculation of the energy (E) of the system as a function of nuclear coordinate (X). Provided with the coupling parameter (H_{ab}) and reorganization energy (λ) for a given MV system ($\Delta G° = 0$ for symmetrical systems), the energies for the ground state (lower surface) and excited state (upper state) are calculated by equations $E_1 = 0.5[\lambda(2X^2 - 2X+1)] - 0.5[\{\lambda(2X - 1)\}^2 + 4(H_{ab})^2]^{1/2}$ and $E_2 = 0.5[\lambda(2X^2 - 2X+1)] + 0.5[\{\lambda(2X- 1)\}^2 + 4(H_{ab})^2]^{1/2}$, respectively.